An Atomic Force Microscopy Study of the Effect of Nanoscale Contact Geometry and Surface Chemistry on the Adhesion of Pharmaceutical Particles

Jennifer C. Hooton,[1,3] Caroline S. German,[2] Stephanie Allen,[1] Martyn C. Davies,[1] Clive J. Roberts,[1,4] Saul J. B. Tendler,[1] and Philip M. Williams[1]

Received November 18, 2003; accepted February 2, 2004

Purpose. To understand differences in particle adhesion observed with increasing humidity between samples of salbutamol sulfate prepared by two different methods.

Methods. Atomic force microscopy (AFM) force measurements were performed as a function of humidity (<10% to 65% RH) using two systems. The first system used clean AFM tips against compressed disks of micronized and solution enhanced dispersion by supercritical fluid (SEDS) salbutamol. The second system involved particles of both salbutamol samples mounted onto the apexes of AFM cantilevers, and force measurements being performed against a highly orientated pyrolytic graphite (HOPG) substrate. Following these measurements, the contact asperities of the tips were characterized.

Results. The first system showed a maximum in the observed adhesion at 22% relative humidity (RH) for the SEDS salbutamol compared to 44% RH for the micronized salbutamol. The second system showed a mix of peaks and continual increases in adhesion with humidity. The predicted Johnson-Kendall-Roberts forces were calculated and divided by the actual forces in order to produce a ratio.

Conclusions. By relating the nature of the asperities to the force measurements, we propose a model in which adhesion scenarios range from single asperity nanometer-scale contact in which peaks in the adhesion were observed, to multiasperity contact where a continuous increase in adhesion was seen with humidity.

KEY WORDS: atomic force microscopy (AFM); contact geometry; humidity; micronized; solution enhanced dispersion by supercritical fluid (SEDS).

INTRODUCTION

In the pharmaceutical industry, a knowledge of particle-particle interaction is important for many processes, such as mixing and flow of powders. It is also important in drug delivery when manufacturing tablets or dry powder inhalers. It is therefore of great interest to be able to understand the adhesion forces between individual particles of a powder.

There are many forces involved in interparticulate adhesion such as van der Waals, electrostatic, and capillary. The major force involved in an interaction will vary according to environmental conditions (1). For example, if the humidity of the environment is low then electrostatic interactions will tend to dominate; however, as the humidity increases, the capillary contribution will become increasingly significant.

Capillary forces arise when a particle and surface approach and moisture condenses in the gap between the two surfaces. This creates a meniscus, which leads to a capillary force between surfaces (2). The value of this force will depend on numerous factors including the surface free energy, surface roughness, gap geometry, surface chemical condition, and the meniscus curvature (2–5). The meniscus curvature is dependent on the relative humidity of the environment, and can be calculated using the Kelvin equation:

$$\left(\frac{1}{r_1}+\frac{1}{r_2}\right)^{-1} = r_K = \frac{\gamma V}{RT\log(p/p_s)} \tag{1}$$

where r_K is the Kelvin radius, V is the molar volume, R is the gas constant, T is the temperature, and (p/p_s) is the relative humidity (2). This can then be used to calculate the effect of the capillary bridge between the two surfaces by consideration of the Laplace pressure. This is calculated using the equation

$$P = \gamma_L\left(\frac{1}{r_1}+\frac{1}{r_2}\right) \tag{2}$$

where P is the Laplace pressure, γ_L is the surface tension of the liquid, r_1 is the concave radius, and r_2 is the contact radius of the meniscus (Fig. 1) (2,5). This pressure acts to pull together an area of πr_2^2. This equation is only true when $r_2 >> r_1$.

In order to understand how environmental conditions affect pharmaceutical particle adhesion, a variety of methods have been used to gain information on the macroscale; for example, the centrifuge technique (6). Recently, the invention of the atomic force microscope (7) has been found to provide additional information on single particle events and how they may affect drug formulations, such as dry powder inhalers (8,9). In these devices, the drug is typically adhered to a larger carrier particle, so that the drug may be entrained in the air stream. Following aerosolization, the drug then separates from the carrier (which impacts upon the back of the throat) and passes into the lungs where it produces its pharmacological effect. Hence, an understanding of the nature and magnitude of forces between the carrier and drug is clearly of significance to developing a successful delivery system, as is indeed a similar understanding of the particles interactions with the various inhaler components.

A recent method of pharmaceutical particle production aimed at tailoring the particle morphology and form has involved the use of supercritical fluids. Supercritical fluids have been used in a number of ways; for example, as solvents (10). A significant advance in this area has been the introduction of the SEDS technique (11), where particle production can be directed by the use of controlled conditions such as flow rate, temperature, and pressure. This can produce uniform particles of controlled size, distribution, and physical properties.

[1] Laboratory of Biophysics and Surface Analysis, School of Pharmacy, University of Nottingham, NG7 2RD, United Kingdom.
[2] Nektar, Bradford, BD7 1HR, United Kingdom.
[3] Current address: Pharmaceutical Technology Research Group, Department of Pharmacy and Pharmacology, University of Bath, BA2 7AY, United Kingdom.
[4] To whom correspondence should be addressed. (email: clive.roberts@nottingham.ac.uk)

ABBREVIATIONS: AFM, atomic force microscopy; DMT, Deryaguin-Muller-Toporov theory; HOPG, highly orientated pyrolytic graphite; JKR, Johnson-Kendall-Roberts theory; SEDS, solution enhanced dispersion by supercritical fluid; RH, relative humidity.

0724-8741/04/0600-0953/0 © 2004 Plenum Publishing Corporation

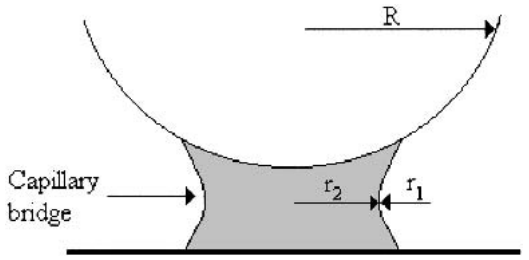

Fig. 1. Formation of a capillary bridge between a particle and substrate.

In this study, the effect of humidity on the adhesion of salbutamol sulfate prepared by micronization and the SEDS technique has been examined. Force measurements against compressed disks of material have been used to generate an understanding of the general behavior of the surfaces, and this has been complemented by force measurements of particles against a flat substrate. To further increase understanding of how capillary forces may affect the obtained adhesion forces, the contact surface of the particles has also been characterized (12).

MATERIALS AND METHODS

The used methods are split into two main areas. The first involved studies of the interaction of blank AFM tips on compressed disks of the micronized and SEDS salbutamol materials as a function of humidity. The second involved the addition of particles onto the apex of AFM tips. Following this, force measurements were performed against an atomically flat substrate, again as a function of humidity.

Measurements of Blank Tips on Compressed Disks

Compressed disks of the micronized salbutamol (BPD sample no. 0141025) and SEDS salbutamol (BPD sample no. 020/99-03) were produced by compressing approximately 100 mg of powder in a 10-mm press dye under vacuum with a force of 10 tons for 5 min. The disks were then mounted onto magnetic stubs using adhesive tape and imaged using tapping mode on a Nanoscope IIIa MultiMode AFM (Veeco, Bicester, UK). Tapping mode imaging was undertaken using silicon TESP tips of nominal spring constant 50 N/m (Veeco) that were plasma-etched prior to imaging with oxygen at 10 W for 30 s in a rf plasma barrel etcher (PT7100, Bio-Rad, Hemel Hempstead, UK). From these images, the root mean square value (R_q) was used to describe the roughness. This value describes the root mean square of the deviation of surface features from the mean line, which is fitted by the calculation of equal areas of the profile being found above and below it. Because roughness can strongly depend on the size of the area being considered (13), the reading is taken from R_q measurements over a range of sample areas ($n = 30$) drawn from within each image. From this, the roughness was then plotted as a function of the side length of each sampling area used.

For force of adhesion measurements, contact cantilevers (Veeco) of nominal spring constant 0.58 N/m were plasma-etched in argon at 10 W for 10 s. Tapping mode tips were also prepared using the same method as the tapping mode imaging tips. To acquire the measurements of the tips on the compressed disks, a molecular force probe (MFP) (Atomic Force F&E GmbH, Mannheim, Germany) was used. The MFP was placed into a sealed container containing desiccant and left for 2 h to equilibrate. Humidity was measured using a humidity probe (HMI 31, Vaisala, Finland), with control being achieved to ±2% RH. The desiccants used were silica gel (Fisher Scientific, Loughborough, UK) for below 10% RH, the saturated salts of potassium acetate (Fisher Scientific) for 22% RH, potassium carbonate for 44% RH (Fluka, Dorset, UK), and sodium chloride for 65% RH (Aldrich, Dorset, UK). It is noted that sodium chloride has an expected saturated RH of 75% RH. However, despite checks to ensure the humidity meter and containment were functioning correctly, the low value we observed does indicate a low level exchange of air with the ambient humidity. Nevertheless, a stable value of 65% RH was continually reached for all experiments with saturated salts of sodium chloride.

Measurements were performed on three different points on each disk for each of the four humidity levels examined. For each measurement, the same contact force and rate of acquisition was used. Approximately 70 force curves were obtained for each measurement. For each humidity, the forces recorded from each point were averaged. From these, bar charts were plotted to show the variation in adhesion with humidity.

Measurements of Particle Against Highly Orientated Pyrolytic Graphite

Particles of the micronized and SEDS salbutamol were added onto plasma etched contact cantilevers following the method described previously (12). Three tips each of the micronized and SEDS salbutamol were made and mounted onto half-moon metal stubs with epoxy adhesive (Araldite, Cambridge, UK) and allowed to dry overnight.

Force measurements were undertaken using a Topometrix Explorer atomic force microscope (Veeco). When the epoxy adhesive had dried, the metal stubs were then mounted onto the atomic force microscope air scanner, which has a Z range of 10 μm. The atomic force microscope was then enclosed in a sealed container, and desiccants were added to control humidity to the values previously stated. Approximately 70 measurements were performed against a substrate of highly orientated pyrolytic graphite (HOPG) (Agar, Stanstead, UK), across a 10 μm × 10 μm area of the substrate for each humidity per tip. The maximum press on force was kept constant at 15 ± 2 nN, and measurements were performed at the same loading rate. Force curves obtained were normal as previously described (12) and showed no long range interaction forces unless otherwise stated.

Once the measurements were obtained, the morphology of the contact region of the tip was characterized using a tip characterization grating (TGT01, NT-MDT, Moscow, Russia), again employing the method previously described (12).

Following characterization, the images were processed using image analysis software (SPIP, Image Metrology ApS, Lyngby, Denmark). Cross sections in both the X and Y direction of a single repeat image of each particles "contact" region were taken as previously described (12) and used to estimate the contact radius of the individual asperities.

Because both samples contain some amorphous material [by dynamic vapor sorption analysis, the micronized salbutamol was shown to contain 6.92% amorphous material, com-

pared to 0.13% for the SEDS (14)], work was undertaken to ensure that no changes in surface structure would occur due to the amorphous regions absorbing water and undergoing recrystallization (15). Due to difficulties in imaging single particles, compressed disks of both salbutamol samples were imaged at <10% RH, 22% RH, 44% RH, and 65% RH to check for changes in surface structure due to the humidity of the environment (results not shown). These images showed no changes in the surface structure, indicating that surface modification due to the presence of moisture was not significant.

Johnson-Kendall-Roberts and Deryaguin-Muller-Toporov Calculations

The Johnson-Kendall-Roberts (JKR) (16) and Deryaguin-Muller-Toporov (DMT) (17) theories were used to calculate the predicted adhesion force from the derived contact radii. The JKR theory calculates adhesion force (F_{ad}) by assuming that surface forces act inside the contact region. It is defined by the equation

$$F_{ad} = \frac{3}{2}\pi\gamma_{ad} R \quad (3)$$

where γ_{ad} is the work of adhesion and R is the radius of the particle.

The DMT theory differs in that it calculates adhesion force by the assumption that surface forces act outside the contact region. This gives the pull of force as -

$$F_{ad} = 2\pi\gamma_{ad} R \quad (4)$$

The work of adhesion for both the JKR and DMT theory was calculated using Eq. 5 (2)

$$\gamma_{ad} = 2\sqrt{\gamma_1\gamma_2} \quad (5)$$

where γ_1 is the apolar surface energy component for the HOPG, which was obtained from Schaefer *et al.* (18), and γ_2 is the apolar surface energy component for either the micronized or SEDS salbutamol particle, taken from Feeley *et al.* (14). For the micronized and SEDS particles, the predicted work of adhesion was calculated as 0.153 Jm^{-2} and 0.124 Jm^{-2}, respectively. The calculated adhesion force values obtained using both theories were then compared to the actual values obtained for adhesion of the particles obtained at <10% RH.

RESULTS

Measurements Obtained Between Blank Tips and Compressed Disks

The roughness profile for both compressed disks is shown in Fig. 2. It is seen that the SEDS salbutamol reached an R_q maximum of 21.8 nm, whereas the micronized material reached a maximum of 12.8 nm. The average of the three measurements of the contact and tapping tips on compressed disks of micronized and SEDS salbutamol are shown in Fig. 3. It is apparent that with both the stiffer tapping cantilevers and the more flexible contact cantilever tips that there is a peak in the interaction at 44% RH for the micronized salbutamol disks and at 22% RH for the SEDS disk. It is noted that the standard deviation for the more flexible contact levers is relatively large. This was due to long-range attractive forces overcoming the lower spring constant of these cantilevers causing them to bend before coming into contact with the sample surface. This was not observed with the stiffer lever due to the larger spring constant making it less sensitive to such forces.

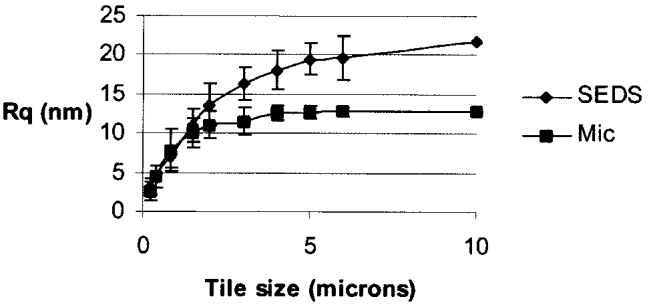

Fig. 2. Surface roughness measurements of SEDS and micronized salbutamol. Measurements were taken using increasing size of sample square.

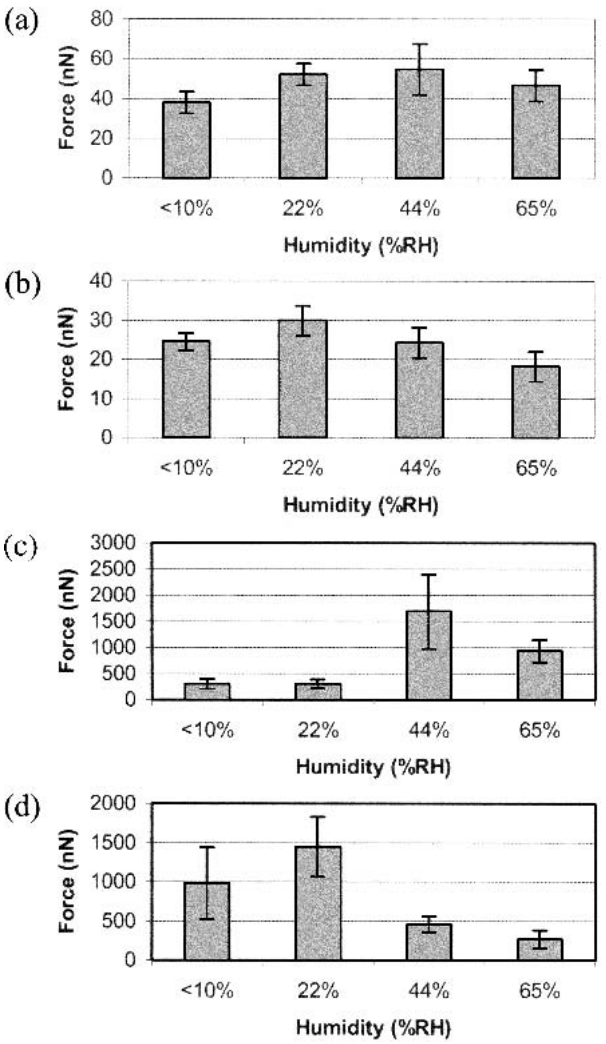

Fig. 3. Force measurements taken using blank AFM tips against compressed disks of SEDS and micronized salbutamol. (a) Flexible contact tip against micronised salbutamol (b) Flexible contact tip against SEDS salbutamol (c) Stiffer tapping tip against micronized salbutamol (d) Stiffer tapping tip against SEDS salbutamol

Measurements Recorded Between Particles and HOPG Substrates

The individual force distributions at each humidity together with the cross sections of the tip used to generate the data are shown in Figs. 4a–4f. For two of the three tips of both the micronized and SEDS salbutamol, similar behavior to the sharp AFM tip on the compressed disk of the respective drug was seen. Two of the three micronized salbutamol tips showed a steady increase in the forces of adhesion measured up until 44% RH before decreasing, whereas two of the three SEDS probes showed an adhesion peak at 22% RH, before a decrease at 44% RH and 65% RH. One of the micronized and SEDS probes showed different behavior in that there was a gradual increase in the adhesion values with humidity, with no peaks observed.

JKR and DMT Forces

The predicted JKR and DMT adhesive forces obtained using the radius calculated for the tip asperities are shown in Tables I and II. It is seen that the JKR forces are closer to the experimentally observed values than the DMT forces. This is expected, as the DMT is more suitable for hard, nondeforming contacts, whereas the JKR model is more suited for contacts where elastic deformation occurs, which is the behavior that would be expected for the HOPG and pharmaceutical particle interaction. To provide a means of comparison of the behavior of the different tips, the calculated JKR value was divided by the observed average force value in order to create a ratio, υ, for each tip.

DISCUSSION

Measurements of Blank Tips on Compressed Disks

The peaks observed in the humidity vs. force plots obtained using a clean sharp AFM tip on compressed disks of micronized and SEDS salbutamol resemble those previously seen in work in which adhesion forces were recorded between a blank tip and flat surfaces of materials such as silica and mica (19,20). In this published work, adhesion measurements were performed using a silicon nitride tip against one of these hydrophilic substrates, at increasing humidity. It was observed that at low humidity levels, a flat region was present in the adhesion data that was attributed to the presence of van der Waals forces only (19). As midrange humidity was reached, a second region was observed where the adhesion force increased. This was considered to be due to the domination of capillary forces following reaching of the critical humidity (19). This region has been observed to occur at a range of values. For example, He *et al.* (19) found it to start at 40% RH for silica; however, for a mica substrate, Xu *et al.* (20) found the increase started at 20% RH.

This adhesion increase region has been interpreted by examination of the lowest height of water film that is required to allow for spreading across a surface (19). This minimum height, e, is calculated using the following equation:

$$e = a_0\left(\frac{\gamma}{S}\right)^{\frac{1}{2}} \tag{6}$$

where γ is the liquid surface tension, S is the spreading coefficient, and a_0 is the molecular length, which is defined by the equation

$$a_0 = \left(\frac{A}{6\pi\gamma}\right)^{\frac{1}{2}} \tag{7}$$

where A the Hamaker constant. S must be zero or positive in order for spreading to occur, and is defined using the equation

$$S = \gamma_{SO} - \gamma_{SL} - \gamma \tag{8}$$

where γ_{SO} is the solid-vacuum interfacial energy and γ_{SL} is the solid-liquid interfacial energy (19). In previous work it has been shown that SEDS salbutamol has a lower surface energy than micronized salbutamol (12,14), which could lead to a lower value of S. This would mean that the minimum height of water required to achieve spreading across the surface would be greater. Because the capillary forces formed at a lower humidity, this must mean that the surface chemistry of the SEDS causes the spreading thickness to be reached at a lower humidity. This would cause the adhesion to the SEDS disk to peak at a lower value of humidity than that of the micronized disk.

Following the increase in the second region, a third distinct region was seen in the adhesion data whereby the forces started to decrease (19). This was attributed to a mixture of attractive and repulsive forces (19). These repulsive forces have been attributed in the literature to one of two reasons. The first involves Laplace pressure. As discussed above, we generally assume $r_2 >> r_1$. However, because a nano-contact is involved, then it is possible that this criteria is not satisfied, leading to a decrease in the Laplace pressure and subsequent decrease in adhesion forces (20). The second explanation involves consideration of chemical potential. Binggeli and Mate (21) described the decrease in adhesion in terms of the chemical potential of liquid in the gap (μ_1) creating an attractive force on the tip. This force (F) is calculated from

$$F = -\frac{\delta G}{\delta z} = -\frac{a}{V}\mu_1 = -\frac{a}{V}kT\ln\left(\frac{p}{p_s}\right) \tag{9}$$

where G is the Gibb's free energy, V is the molar volume, z is the distance between sample surface and tip, a is the area of the liquid, and k is the Boltzmann constant. This equation indicates that as relative humidity increases, the force due to the water in the gaps becomes more repulsive consistent with the observed reduction in adhesion (21).

It should be noted that the two salbutamol surfaces had a difference in surface roughness when larger sample dimensions were used. This will affect the results because according to Coelho and Harnby (22), the thickness of layer of adsorbed water on the surface of the disk (e) would decrease by an amount equal to half the average peak to trough height. Because the SEDS disk was rougher, this would mean that the wetting of the surface would be hindered more than the micronized surface. However, despite this, our data clearly illustrate through a later onset of an adhesion maxima that the micronized system still exhibited a lower level of wetting.

Particles on HOPG Surface

In order to explain the results obtained for the SEDS and micronized material on HOPG, some of the previous argu-

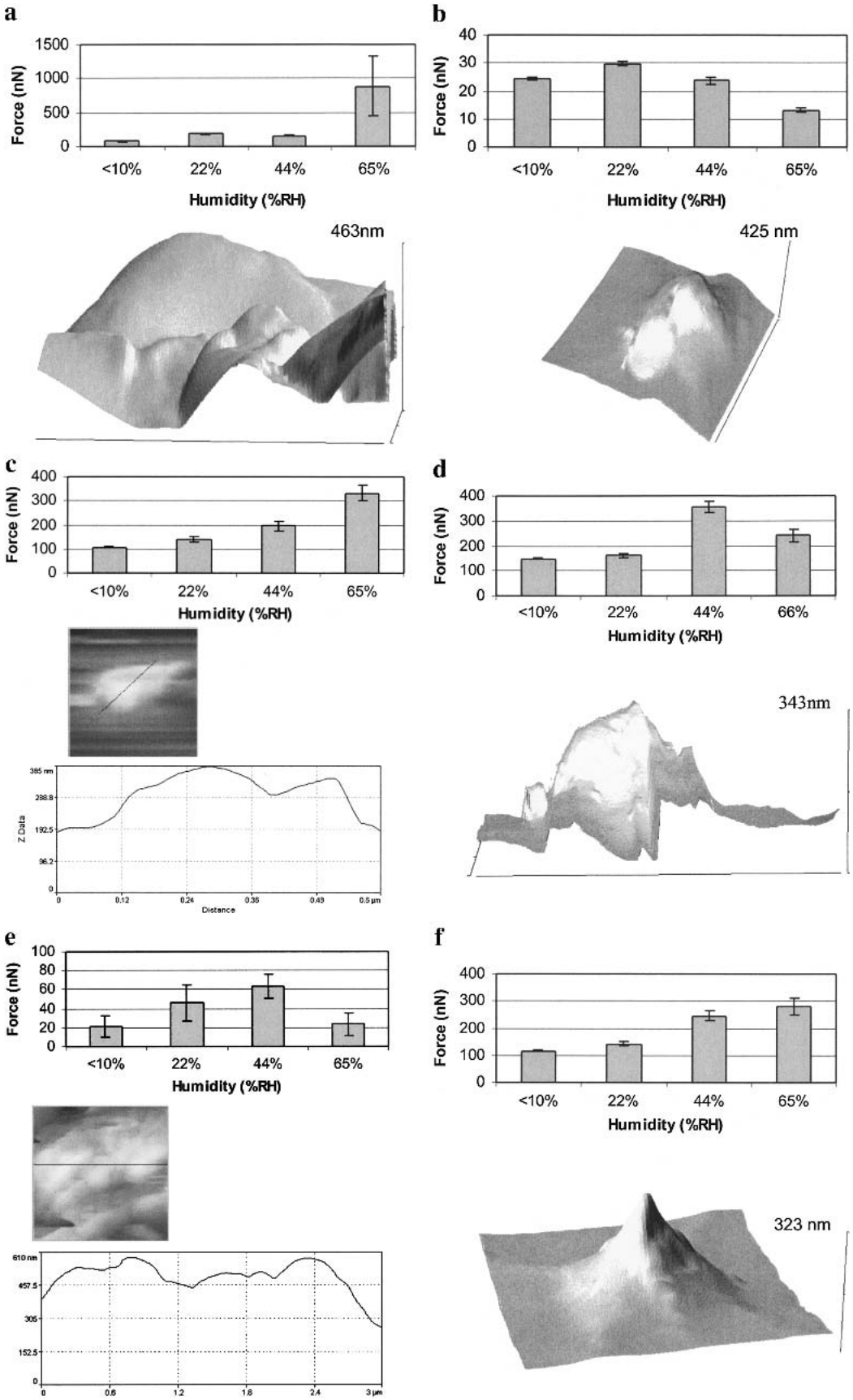

Fig. 4. Force distribution for changing humidity and contact surface images of tips used. (a) SEDS salbutamol tip one, XY = 1.45 μm, Z = 409 nm. (b) SEDS salbutamol tip two, XY = 1.25 μm, Z = 407 nm. (c) SEDS salbutamol tip three, XY = 1.2, μm Z = 396 nm. (d) Micronized salbutamol tip one, XY = 1.3 μm, Z = 333 nm. (e) Micronized salbutamol tip two, XY = 2.51 μm, Z = 559 nm. (f) Micronized salbutamol tip three, XY = 1.2 μm, Z = 314 nm.

Table I. Table of Actual Forces Obtained at <10% RH, Forces Calculated Using the JKR and DMT Theories, and υ Value for SEDS Salbutamol Tips (Standard Deviation in Parentheses)

Tip	Actual force (nN)	JKR prediction (nN)	DMT prediction (nN)	υ
Tip one	78.43 (4.69)	587.5	783.67	7.52
Tip two	24.47 (0.64)	170	226.7	7.08
Tip three	106.39 (1.39)	128	170.6	1.20

RH, relative humidity; JKR, Johnson-Kendall-Roberts; DMT, Deryaguin-Muller-Toporov; SEDS, solution enhanced dispersion by supercritical fluid.

Table II. Table of Actual Forces Obtained at <10% RH, Forces Calculated Using the JKR and DMT Theories, and υ Value for Micronized Salbutamol Tips (Standard Deviation in Parentheses)

Tip	Actual force (nN)	JKR prediction (nN)	DMT prediction (nN)	υ
Tip one	148.98 (3.18)	274	365	1.84
Tip two	21.49 (11.58)	129	172	6.14
Tip three	116.50 (3.23)	144	192	1.24

RH, relative humidity; JKR, Johnson-Kendall-Roberts; DMT, Deryaguin-Muller-Toporov; SEDS, solution enhanced dispersion by supercritical fluid.

ments can be extrapolated so that a model of adhesion for the particles, which encompasses different contact geometry, can be proposed. In this model, we propose that there are three scenarios for the interaction being studied here. The first is shown in Fig. 5a. Here, there is a single point of adhesion, similar to that of a sharp blank AFM tip on a compressed disk of material. The nanoscale contact geometry and surface chemistry discussed for the tip on compressed disk will lead to a clearly defined peak in the humidity profile. Such behavior, which we term Contact Scenario One, is seen in three of the tips discussed here, namely micronized tip one (Fig. 4d) and SEDS tips one (Fig. 4a) and two (Fig. 4b).

For micronized tip one, it is seen that there is a peak at 44% RH. This is the same humidity that the peak in the tip on compressed disk is seen, indicating that the surface chemistry may be dominating the interaction. When the tip image is examined, it is seen that the interacting area of micronized tip one consists of a single asperity, which would be expected for a Contact Scenario One situation.

If SEDS tips one and two are examined, it is observed that there is a gradual increase in adhesion force up to 22% RH before a decrease at 44% RH. Because a similar peak in adhesion force was seen at 22% RH with the tip on compressed disk, this again indicates that it is the surface chemistry of the SEDS material that is dominating the interaction. For tip two this decrease continues at 65% RH, which again

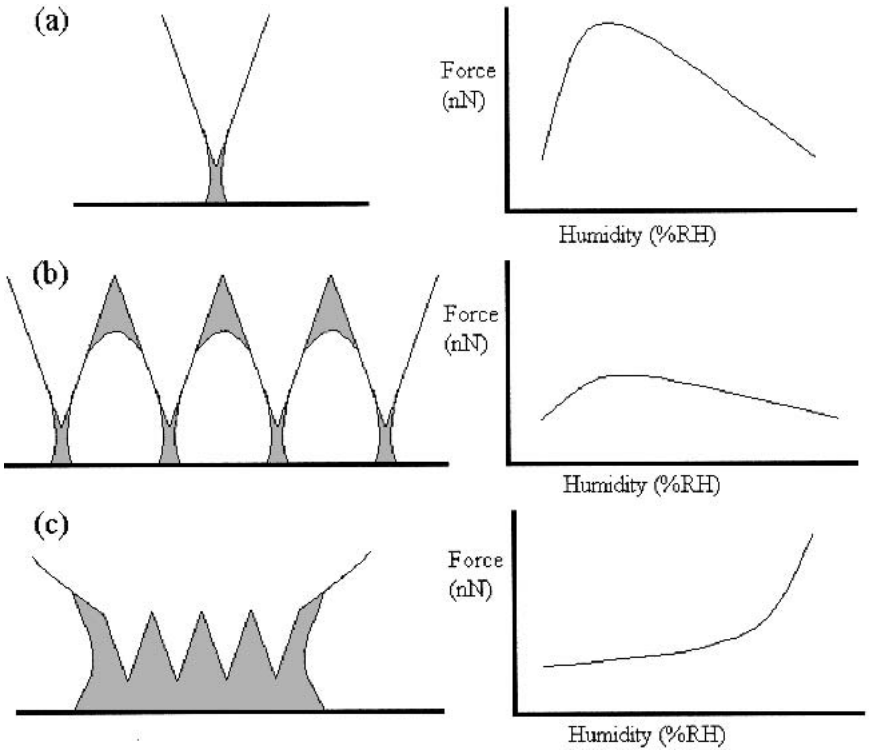

Fig. 5. The three scenarios of adhesion and how they correspond to behavior. (a) Contact Scenario One: a single asperity is in contact with the surface. This leads to a clearly defined peak in adhesion force. (b) Contact Scenario Two: multiple nanoscale asperities contacting the surface. Moisture begins to condense between the gaps but is not sufficient to saturate the individual asperities. This leads to a peak effect, however, it is more depressed than that seen for scenario one. (c) Contact Scenario Three: saturation of asperities leading to larger contact area. This leads to a gradual increase in adhesion force with humidity.

is accounted for by a singe asperity coming into contact with the surface.

However, for SEDS tip one at 65% RH, there is a large rise in force. At this humidity, the force curves show a similar appearance to curves that would be seen for the presence of a liquid neck (23,24). The large increase seen at 65% RH for tip one may be due to a sudden dominance of capillary forces. This can be explained by considering the image of the asperity coming into contact. The image shows that there are two distinct asperities, which differ in height by 59 nm. At the lower humidity, only the larger of the two asperities will be involved in the interaction. At 65% RH, the thickness of the water layer on HOPG is approximately 34 nm (25), which, when combined with the water layer on the particle, means that the second peak will become involved in the interaction. The gap between the two asperities was found to have a maximum depth of 94 nm and which could have become filled by liquid due to spontaneous condensation (2), leading to an increase in the capillary force and hence the observed adhesion force.

The contact geometry conditions for Contact Scenario Two are shown schematically in Fig. 5b. Here, the particle has multiple asperities, instead of a single asperity, adhering to the substrate. At higher humidity, the gaps in-between the asperities are not completely filled with moisture. The presence of multiple, nanoscale contact points will produce a peak effect, however they will also trap more moisture in the gap between asperity and substrate at lower humidity, leading to a greater repulsive force as explained by the chemical potential theory (21). This repulsive force will then cause the peak effect to be masked.

Contact Scenario Two behavior is only seen with micronized tip two (Fig. 4e) where there is less distinction between the forces at the different humidity levels than for micronized tip one. Micronized tip two has numerous asperities, with the vertical distance between the two highest asperities being only 4 nm, while the trough depth is 115 nm. The peak effect could thus be due to the two larger asperities coming into contact with the substrate.

When the force is examined with measurement number, it is seen that at 44% RH there is a gradual decrease in forces as the measurements progressed. Podczeck (1,26) has observed that at humidity levels below 55% RH, plasticizing of the surfaces may occur due to adsorbed moisture, which could imply humidity dependent plastic changes in the sample were occurring at 44% RH. However, this is unlikely here because when imaging the compressed disks at varied humidity, no changes in surface structure where seen. In addition, the decrease in force with progressive measurements was not observed at 65% RH.

The contact geometry conditions for Contact Scenario Three is shown in Fig. 5c. In this scenario, the asperities have smaller dimensions, and hence the gaps between them become saturated before a peak effect is seen. This means that any single, nano contacts are lost at a lower humidity, and there is only one large area involved in the interaction. This changes the behavior from a nanoscale contact to a macroscale contact, where adhesion forces increase with humidity and no peak effect is seen.

If SEDS tip three (Fig. 4c) is considered, there is a gradual increase in adhesion forces as the humidity increases. If the tip image is studied, then it is apparent that the particle adhered has many asperities separated from the highest asperity by distances of between 50 and 56 nm. The troughs in-between these asperities vary in depth from 50 to 72 nm. At 44% RH, a gradual increase in the adhesion force with the number of measurements taken was observed. This is related to the more numerous, smaller voids in between the asperities, which could have become filled with moisture, leading to an increase in capillary force. This gradual increase in peaks contacting the surface masks the peak effect expected at 22% RH.

Micronized tip three (Fig. 4f) also shows a continual increase in force with increasing humidity. However, it can be seen that the force at 44% RH shows a much bigger increase than that seen between <10% and 22% RH. This again could be surface chemistry dominated. At 65% RH, the force continues to increases. The shape of the asperity again can be used to explain this. When observing tip three, scenario one behavior would be expected as it is a single asperity. However, if its dimensions are compared to micronized tip one, it is seen that though the height is similar, tip three has a much narrower geometry. This means that the asperity has been saturated by surface water at 65% RH leading to the observed continual increase in force.

Though numerous other groups are using the atomic force microscope to perform particle force measurements, to the best of the authors' knowledge, this peak effect has not been reported with pharmaceutical materials before, although previous work has mainly focused on interactions with non-atomically flat surfaces (8,9,27). A recent study was performed by Price *et al.* (28) using salbutamol against a lactose crystal whose surface had been modified to produce nanoscale roughness, although this work did not show a peak effect, and instead adhesion increased with humidity. It should also be noted that no attempt has made to characterize the contacting asperities in previously undertaken work, so direct comparisons cannot be made to the data presented in this paper. However, in subsequent work undertaken by the author, it was shown that the peak effect could be reproduced with other drug substances (29).

It is also worthy of note that this study has highlighted some of the complexities needed to be considered when interpreting the apparently straightforward AFM measurement of an adhesion force between particles. The need to account for the significant morphological and chemical heterogeneity at the nanoscale displayed by real materials is a significant challenge that, though addressed here, still needs to be fully addressed both theoretically and experimentally.

JKR Forces

When the υ values of the SEDS material are examined in Table I, it is noted that tips one and two, where a peak is seen at 22% RH, have a larger υ value than that of the tip three, where no peak was seen. This may be due to one of two reasons. The first of which is that there are surface features that are too fine to be imaged by the tip characterizer, meaning that at lower humidity levels, the contact region is smaller then that calculated using the images.

The second reason is that the surface chemistry may also be involved. Schaefer *et al.* (18) performed similar calculations between HOPG surfaces and glass, tin, and polystyrene surfaces. It was found that the JKR forces were 40 to 68 times

higher than the observed values, which was mainly attributed to surface roughness effects. Following an allowance for this prediction, forces were still three times greater than observed (18). This was accounted for by small layers of moisture that could not be removed by vacuum and by variations in the interfacial energies. However, in our study, the tip on compressed disk adhesion data show that the SEDS material is more sensitive to moisture at a lower humidity than the micronized material. This indicates that a larger water layer was present on the SEDS material even at low humidity, which could lead to the generation of a disjoining pressure caused by water in the meniscus (1). This would also assist in keeping the asperities away from the surface and hence deviation from predicted values. Tip three had a lower υ value, which suggests that the calculation of contact radius may have been underestimated due to the large number of asperities present.

When the υ values for the micronized salbutamol in Table II are examined, it is seen that for tips one and three, there is a lower υ value. This could be accounted for by a better characterization of the asperity coming into contact with the surface, as well as the knowledge that at lower humidity levels, the micronized salbutamol was less sensitive to moisture, meaning that there was a lower disjoining pressure present. For tip 2 it is observed that there is a larger υ value. This could be due to the difficulties in predicting which asperities would be coming into contact with the substrate surface and inconsistent interfacial energy leading to a incorrect prediction of contact area and thus JKR calculation.

CONCLUSIONS

In this work, a comparison in the behavior of SEDS and micronized salbutamol in two different experimental systems (particle on HOPG and AFM tip on salbutamol disks) at a range of humidity levels was made.

When force measurements of a blank AFM tip against compressed disks of both materials were made, it was observed that for the SEDS material there was a peak in adhesion at 22% RH, whereas for the micronized material this peak was at 44% RH. This was attributed to different wetting effects of both materials, possibly due to surface chemistry differences.

When particles of both the materials were added onto the end of AFM cantilevers and force measurements were performed against a HOPG substrate at the same range of humidity levels, a mixture of behaviors were observed. This was explained by a model that considered the contact geometries in three separate scenarios in which the contact asperities change from single nano contacts (Contact Scenario One), to multiple contacts where the asperities are not filled with moisture (Contact Scenario Two), to saturation of these to form a larger macro contact (Contact Scenario Three). This model leads to a gradual change from the peak in the adhesion with humidity, as also seen with a blank tip on a compressed disk of material, to a continual increase in force with humidity.

When the υ values were calculated (ratio of calculated JKR value divided by the observed average force value), it was seen that the SEDS material had a higher deviation from the theoretical adhesion force than the micronized. This was explained by the SEDS being more sensitive to lower humidity levels than the micronized material.

This work has shown that when considering individual particles, differences in surface chemistry and asperity geometry can lead to drastic changes in adhesion with different humidity conditions. This observation shows that the interpretation of the apparently straightforward AFM measurement of particle adhesion force needs to take account of these factors if meaningful conclusions are to be drawn of direct benefit to formulation design and delivery. Though it must be remembered that this work was undertaken against a model substrate, and that there are numerous other factors to be considered in the formulation of inhalers, the data presented here suggests that at higher humidity levels, adhesion may be reduced by the use of particles with numerous, well-defined asperities in a system similar to that seen in Contact Scenario Two. Such particle engineering would lead to the avoidance of maxima in adhesion with humidity and depressed forces through the humidity range, meaning that a more predictable release of drug may be achieved.

ACKNOWLEDGMENTS

J. C. H. would like to acknowledge Nektar and the Biotechnology and Biological Sciences Research Council for studentship funding.

REFERENCES

1. F. Podczeck, J. M. Newton, and M. B. James. The influence of constant and changing relative humidity of the air on the autoadhesion force between pharmaceutical powder particles. *Int. J. Pharm.* **145**:221–229 (1996).
2. J. N. Israelachvili. *Intermolecular and Surface Forces*, Academic Press Inc., London, UK, 1991.
3. F. Podczeck. *Particle-particle Adhesion in Pharmaceutical Powder Handling*, Imperial College Press, London, 1998.
4. A. Marmur. Tip-surface capillary interactions. *Langmuir* **9**:1922–1926 (1993).
5. R. Jones, H. M. Pollock, J. A. S. Cleaver, and C. S. Hodges. adhesion forces between glass and silicon surfaces in air studied by afm: effects of relative humidity, particle size, roughness, and surface treatment. *Langmuir* **18**:8045–8055 (2002).
6. F. Podczeck. Assessment of the mode of adherence and the deformation characteristics of micronized particles adhering to various surfaces. *Int. J. Pharm.* **145**:65–76 (1996).
7. G. Binnig, C. F. Quate, and C. Gerber. Atomic force microscope. *Phys. Rev. Lett.* **56**:930–933 (1986).
8. J. K. Eve, N. Patel, S. Y. Luk, S. J. Ebbens, and C. J. Roberts. A study of single drug particle adhesion interactions using atomic force microscopy. *Int. J. Pharm.* **238**:17–27 (2002).
9. P. M. Young, R. Price, M. J. Tobyn, M. Buttrum, and F. Dey. Investigation into the effect of humidity on drug-drug interactions using the atomic force microscope. *J. Pharm. Sci.* **92**:815–822 (2002).
10. J. W. Tom and P. G. Debenedetti. Formation of bioerodible polymeric microspheres and microparticles by rapid expansion of supercritical solutions. *Biotechnol. Prog.* **7**:403–411 (1991).
11. P. York. Strategies for particle design using supercritical fluid technologies. *PSTT* **2**:430–440 (1999).
12. J. C. Hooton, C. S. German, S. Allen, M. C. Davies, C. J. Roberts, S. J. B. Tendler, and P. M. Williams. Characterization of particle interactions by atomic force microscopy: effect of contact area. *Pharm. Res.* **20**:508–514 (2003).
13. J. D. Kiely and D. A. Bonnell. Quantification of topographic structure by scanning probe microscopy. *J. Vac. Sci. Technol. B* **15**:1483–1493 (1997).
14. J. C. Feeley, P. York, B. S. Sumby, and H. Dicks. Comparison of the surface properties of salbutamol sulphate prepared by micronization and a supercritical fluid technique. *J. Pharm. Pharmacol.* **50**:S54 (1998).
15. G. H. Ward and R. K. Schultz. Process-induced crystallinity

changes in albuterol sulfate and its effect on powder physical stability. *Pharm. Res.* **12**:773–779 (1995).
16. K. L. Johnson, K. Kendall, and A. D. Roberts. Surface energy and the contact of elastic solids. *Proc. R. Soc. Lond. A* **324**:301–313 (1971).
17. B. V. Derjaguin, V. M. Muller, and Y. P. Toporov. Effect of contact deformations on the adhesion of particles. *J. Colloid Interface Sci.* **53**:314–326 (1975).
18. D. M. Schaefer, M. Carpenter, B. Gady, R. Reifenberger, L. P. Demejo, and D. S. Rimai. Surface roughness and its influence on particle adhesion using atomic force techniques. *J. Adhesion Sci. Technol.* **9**:1049–1062 (1995).
19. M. He, A. S. Blum, D. E. Aston, C. Buenviaje, and R. M. Overney. Critical phenomena of water bridges in nanoasperity contacts. *J. Chem. Phys.* **114**:1355–1360 (2001).
20. L. Xu, A. Lio, J. Hu, D. F. Ogletree, and M. Salmeron. Wetting and capillary phenomena of water on mica. *J. Phys. Chem. B* **102**:540–548 (1998).
21. M. Binggeli and C. M. Mate. Influence of capillary condensation of water on nanotribology studied by force microscopy. *Appl. Phys. Lett.* **65**:415–417 (1994).
22. M. C. Coelho and N. Harnby. Moisture bonding in powders. *Powder Technol.* **20**:201–205 (1978).
23. N. A. Burnham, R. J. Colton, and H. M. Pollock. Interpretation of force curves in force microscopy. *Nanotechnology* **4**:64–80 (1993).
24. F. K. Dey, J. A. S. Cleaver, and P. A. Zhdan. Atomic force microscopy study of adsorbed moisture on lactose particles. *Adv. Powder Technol.* **11**:401–413 (2000).
25. J. Freund, J. Halbritter, and J. K. H. Horber. How dry are dried samples? water adsorption measured by STM. *Micr. Res. Tech.* **44**:327–338 (1999).
26. F. Podczeck, J. M. Newton, and M. B. James. Variations in the adhesion force between a drug and carrier particles as a result of changes in the relative humidity of the air. *Int. J. Pharm.* **149**: 151–160 (1997).
27. V. Berard, E. Lesniewska, C. Andres, D. Pertuy, C. Laroche, and Y. Pourcelot. Affinity scale between a carrier and a drug in DPI studied by atomic force microscopy. *Int. J. Pharm.* **247**:127–137 (2002).
28. R. Price, P. M. Young, S. Edge, and J. N. Staniforth. The influence of relative humidity on particulate interactions in carrier-based dry powder inhaler formulations. *Int. J. Pharm.* **246**:47–59 (2002).
29. J. C. Hooton. PhD Thesis, University of Nottingham, Nottingham, UK, 2003.